

One-Electron and Phonon-Assisted Tunneling in *n*-Ge Schottky Barriers*

L. C. DAVIS†† AND F. STEINRISSER‡

Department of Physics and Coordinated Science Laboratory, University of Illinois, Urbana, Illinois 61801

(Received 2 June 1969)

The experimental tunneling conductance of metal-Ge contacts is compared to the predictions of the one-electron Schottky-barrier model in which all parameters are determined from experiments other than tunneling. Agreement is found in the magnitude and the shape of conductance-versus-bias curves for vacuum-cleaved Sb-doped Ge units. The qualitative features of the As-doped units are also in agreement, but a discrepancy in magnitude exists. Substantially larger conductance is found in air-cleaved junctions than in vacuum-cleaved junctions. Capacitance measurements reveal that the barrier height for air-cleaved junctions is $V_b=0.51$ V, whereas $V_b=0.63$ V for vacuum-cleaved junctions. Pronounced step increases in the conductance due to phonon-assisted tunneling occur at $eV=\pm\hbar\omega$, where $\hbar\omega$ is the energy of a Ge phonon at the Brillouin-zone boundary along the [111] direction. Structure is clearly observed at all four phonon energies (TA, LA, LO, TO). The magnitude of the LA phonon-assisted tunneling is accounted for in a theoretical calculation based upon a mechanism suggested by Kleinman to explain similar phenomena in Ge *p-n* junctions. The strengths of the TA and LO phonon-assisted tunneling also appear to be in reasonable agreement with qualitative considerations, but the observed TO phonon-assisted tunneling is stronger than expected.

I. INTRODUCTION

A CALCULATION of the tunneling conductance as a function of bias voltage for a metal-semiconductor junction has been given by Conley, Duke, Mahan, and Tiemann (CDMT).¹ This calculation was based upon the Schottky model with a parabolic potential for the barrier. Specular reflection at the metal-semiconductor interface was assumed. The mobile charge carriers of the highly doped degenerate *n*-type semiconductor electrode were taken to behave as a free-electron gas with Fermi energy $e\mu_F$ (Fermi level $e\mu_F$ above conduction band edge) at $T=0^\circ\text{K}$ and an effective mass m_e^* . The first comparison of experimental data to the CDMT calculation was given by Conley and Tiemann.² They found favorable agreement (but with some discrepancies) for chemically prepared diodes made from degenerate *n*-type Ge and either Au or In as the metal electrode. Subsequently, it was shown³ that the technique of evaporation of metal electrodes on vacuum-cleaved Sb-doped Ge surfaces gave greatly improved agreement with theory. It was concluded that the absolute magnitude, as well as the shape of the experimental curve, was adequately described by the one-electron theory of Schottky-barrier tunneling with all parameters in the calculation determined from experiments other than tunneling.³ The agreement in As-doped Ge units, however, was not as good as in Sb-doped units.

The purpose of the first part of this paper is to discuss the comparison of Sb-doped units to theory with a more accurate measurement of the carrier density, to present data for As-doped units, and to describe the effects of air cleavage on both the tunneling conductance and the barrier heights (as determined from capacitance measurements).

In the second part of the paper, we discuss the step increases in the conductance due to strong phonon-assisted tunneling observed in both Sb-doped and As-doped metal-Ge junctions. This inelastic tunneling process involves the emission of Ge phonons of all four branches (transverse acoustic=TA, longitudinal acoustic=LA, longitudinal optic=LO, transverse optic=TO) at the Brillouin-zone-boundary along the [111] axis. These are the same phonons as observed in Sb-doped Ge *p-n* junctions⁴ where the emission of zone-boundary phonons along the [111] axis is required for momentum conservation in an indirect diode (in the absence of appreciable impurity scattering which obscures the phonon effects in As-doped Ge *p-n* junctions⁵). In the metal-semiconductor contact, we find that the same momentum conservation rule applies to electrons with small $k_{||}$ in the metal. A calculation of the strength of the LA phonon-assisted tunneling in the metal-semiconductor contact based upon a modification of Kleinman's theory⁶ for indirect *p-n* junctions is described in Sec. IV. As previously noted,³ the Kleinman mechanism is a two-step process of an electron first tunneling from the metal (in reverse bias) into an evanescent state associated with the electronic spectrum at Γ_2' in the Ge Brillouin zone, and then emitting a phonon and being scattered into a current-carrying state at L_1 .

* Work supported in part by the National Aeronautics and Space Administration under Grant No. NsG 228-62, by the Joint Services Electronics Program, Army Contract No. DAAB-07-67-C0199, and by the U. S. Army Research Office (Durham) under Contract No. DA-31-124-ARO(D)-114.

† National Science Foundation Post doctoral Fellow.

‡ Present address: Scientific Laboratory, Ford Motor Company, Dearborn, Mich., 48121.

¹ J. W. Conley, C. B. Duke, G. D. Mahan, and J. J. Tiemann, *Phys. Rev.* **150**, 466 (1966).

² J. W. Conley and J. J. Tiemann, *J. Appl. Phys.* **38**, 2880 (1967).

³ F. Steinrisser, L. C. Davis, and C. B. Duke, *Phys. Rev.* **176**, 912 (1968).

⁴ R. T. Payne, *Phys. Rev.* **139**, A570 (1965). (Additional references can be found in this reference.)

⁵ H. Holonyak, Jr., I. A. Lesk, R. N. Hall, J. J. Tiemann, and H. Ehrenreich, *Phys. Rev. Letters* **3**, 167 (1959).

⁶ L. Kleinman, *Phys. Rev.* **140**, A637 (1965).

II. EXPERIMENTAL TECHNIQUE

A. Contact Preparation

Single crystal bars of *n*-type Ge doped to an impurity concentration of approximately $7 \times 10^{18}/\text{cm}^3$ with As or Sb were cut with the long axis in the $[100]$ direction. The sample size was $10 \times 4 \times 2$ mm. After being cut, the samples were etched in CP-4.

Ohmic contacts were attached to the bars by soldering copper wires with an In-Sn solder to them. Bars which had two such contacts were checked at 4.2°K. The contacts were Ohmic and exhibited a very low resistance.

Tunneling contacts were made by cleaving the bars in a vacuum of 1×10^{-7} Torr after scribing them in the middle with a diamond. A few seconds after cleavage, a stainless-steel mask was brought close to the (100) cleavage plane. A shutter between the evaporation source and the sample was opened. 99.999% pure In or 99.99% pure Pb was evaporated from alumina-coated wire baskets. The evaporation was started about 1 min before cleavage such that the evaporation rate had stabilized at 50 Å/sec at the time of cleavage. Dots of 2.5×10^{-4} - and 5×10^{-5} -cm² area were evaporated to a thickness of ~ 5000 Å as monitored by a quartz crystal deposition monitor.

Contacts to the In or Pb dots were made by pressing a freshly cut In wire tip into a dot located on a good cleavage area. Cold welding produced satisfactory electrical and mechanical contacts.⁷

B. Low-Temperature Measurements

Tunneling measurements were performed in a helium immersion Dewar. Temperatures below 4.2°K were obtained by pumping on the liquid helium. The lowest temperature was 1.8°K. A calibrated Ge thermometer was used for temperature measurements. A Cartesian manostat inserted in the helium pump line kept the temperature constant to better than 1%.

The occurrence of tunneling was confirmed by the observation of the superconducting energy gap in the contact metal below its critical temperature, i.e., 3.4°K for In and 7.2°K for Pb, respectively.

C. Electronics

Conductance, dI/dV , and second derivative, d^2I/dV^2 , measurements were made according to standard techniques.⁸ Figure 1 shows schematically the setup which is approximately the same as the one shown in Fig. 6 of Ref. 4. The dc source which could be swept electronically from -6 to $+6$ V was a transistorized power supply fed by two wet cells. The dc source was shunted by a resistor R_{dc} of 2 Ω in series with a resistor R_s of 1 or 0.1 Ω. The ac modulation at a frequency $f = 1000$ cps was supplied

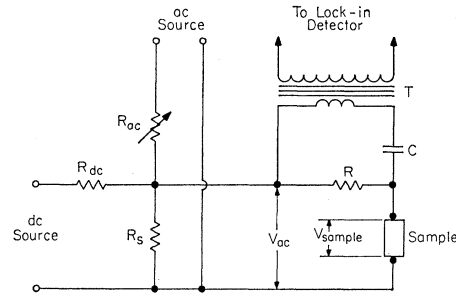


FIG. 1. Schematic drawing of the circuit used to measure dI/dV and d^2I/dV^2 .

by an audio generator. It was shunted by a variable resistor $R_{ac} < 1$ kΩ in series with R_s . R_{dc} and R_{ac} serve to decouple dc and ac sources from each other. R_s determined the source resistance seen by the junction. R_s assured a constant ac level for varying junction resistance as long as it was chosen much smaller than the junction resistance.

The dc and ac voltage developed across R_s was applied through a sampling resistor R to the tunneling junction. The ac current $I(f)$ and $I(2f)$ at the frequencies f and $2f$, respectively, flowing through R was converted into a voltage which was fed through a capacitor C into a transformer T . The voltage was amplified and detected by a lock-in detector.

According to Ref. 4, the currents $I(f)$ and $I(2f)$ are related to dI/dV and d^2I/dV^2 as follows:

$$I(f) = \frac{dI}{dV} \left(1 + \frac{dI}{dV} R \right)^{-1} V_{ac} + \text{const} \frac{d^3I}{dV^3} V_{ac}^3, \quad (2.1)$$

$$I(2f) = (2)^{-3/2} \frac{d^2I}{dV^2} \left(1 + \frac{dI}{dV} R \right)^{-3} V_{ac}^2 + \text{const} \frac{d^4I}{dV^4} V_{ac}^4. \quad (2.2)$$

In this case, R is the value of the sampling resistor (R in Fig. 1) plus the lead resistance, and V_{ac} is the ac amplitude measured across R_s .

The values of R were chosen such that $(dI/dV)R \ll 1$. The maximum dI/dV measured was $5 \times 10^{-2} \Omega^{-1}$ for which R was 0.5 Ω, so that $(dI/dV)R = 2.5 \times 10^{-2}$. The amplitude V_{ac} was small enough that the contributions due to higher-order terms were negligible. Consequently, dI/dV and d^2I/dV^2 were proportional to $I(f)$ and $I(2f)$, respectively. Calibration of dI/dV was done by replacing the sample by a precision resistance decade. The lead resistance was less than 0.4 Ω and could be neglected.

D. Barrier Heights

The barrier height V_b was determined by measuring junction capacitance C -versus-bias voltage V at 77°K with a Boonton 33A rf admittance bridge. The fre-

⁷ We are indebted to E. L. Wolf for discussing this technique.

⁸ J. G. Adler and J. E. Jackson, Rev. Sci. Instr. 37, 1049 (1966).

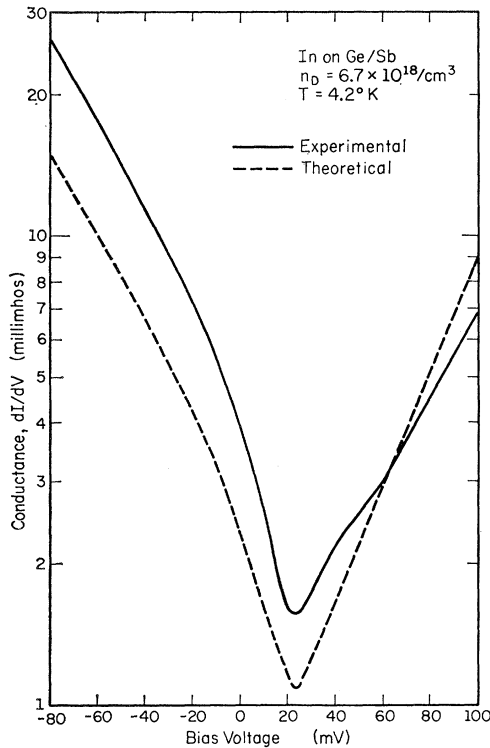


FIG. 2. Comparison between experimental conductance-versus-voltage curve (solid line) on $n_D = 6.7 \times 10^{18}/\text{cm}^3$ Sb-doped Ge at 4.2°K and the conductance calculated according to the model developed in Ref. 1 (dashed line). The contact metal is In. The contact area is $2.5 \times 10^{-4} \text{ cm}^2$, and the barrier height is 0.63 V. The Fermi degeneracy $\mu_F = 23 \text{ mV}$.

quency was 1 MHz, and the modulation amplitude was 5 mV. The capacitance C of a metal-degenerate semiconductor contact is given by⁹

$$C = A [e^2 \epsilon_s n_D / 8\pi (eV_b + \frac{3}{5} e\mu_F - eV)]^{1/2}, \quad (2.3)$$

where A is the junction area, e the electron charge, ϵ_s the static dielectric constant of the semiconductor, n_D the number of free carriers per unit volume, V_b the barrier height, μ_F the Fermi degeneracy of the semiconductor, and V the applied bias. In this paper, the sign convention for V is that $V > 0$ when the metal is positive with respect to the n -type semiconductor which is opposite to the sign convention in Ref. 3.

By plotting $1/C^2$ versus V , one obtains a straight line whose intersection with the V axis determines $eV_b + \frac{3}{5} e\mu_F$. For vacuum-cleaved contacts, it was found that $V_b = 0.63 \pm 0.03 \text{ V}$. V_b was found to be independent of the contact metal (In or Pb) and independent of the dopant of the semiconductor (Sb or As). For air-cleaved junctions, the value of V_b was found to be $0.51 \pm 0.03 \text{ V}$. Within experimental error, the junction capacitance values at fixed bias voltages agreed with Eq. (2.3). Curves of $1/C^2$ versus V were slightly concave but

⁹ J. W. Conley and G. D. Mahan, Phys. Rev. **161**, 681 (1967). Equation (4.1) of this reference contains a typographical error. Equation (2.3) of this paper is the correct result.

they could be closely approximated by straight lines. The largest uncertainty was in the determination of the junction area, this uncertainty amounting to about 20%. This was due to poorly defined edges of the evaporated dots caused by the separation of the evaporation mask from the sample during evaporation and by the finite size of the evaporation source.

E. Carrier Concentrations

Carrier concentrations were determined by measuring Hall coefficients on clover-leaf samples $\frac{1}{8}$ in. in diameter. The Hall samples were cut from the tunneling bars. Measurements were performed at room temperature and at 77°K and gave identical results within experimental error ($\approx 1\%$). Bulk resistivities were also obtained from these measurements. Bulk resistivities and Hall coefficients agree well with the published data of Spitzer *et al.*¹⁰

III. EXPERIMENTAL RESULTS AND COMPARISON WITH THEORY

A. Conductance-Versus-Voltage Curves

In Ref. 2, curves of differential resistance dV/dI -versus- V were displayed which showed an order-of-magnitude agreement with the theory developed in Ref. 1. The agreement in curve shape, absolute value and position of the resistance maximum was considered to be satisfactory. The discrepancies observed were attributed to shortcomings in the theory such as the omission of band tailing.² Our results indicate that improved diode fabrication techniques give much better agreement between experiment and the theory of Ref. 1, particularly for Sb-doped Ge. The agreement in the case of As-doped Ge, however, is not as good.

1. Results for Sb-doped Ge

In Fig. 2, curves of conductance dI/dV versus voltage at $T = 4.2^\circ\text{K}$ are displayed for an indium contact on Sb-doped Ge (solid line). This is one typical curve out of 12 curves of which the high and low extremes and the most commonly observed curves were displayed in Fig. 1 of Ref. 3. The dashed curve in Fig. 2 is a theoretical calculation based on the CDMT theory.¹ The following experimentally determined parameters were used in the calculation: carrier density $n_D = (6.7 \pm 0.1) \times 10^{18}/\text{cm}^3$,¹¹ barrier height $V_b = 0.63 \pm 0.03 \text{ V}$, and junction area $A = (2.5 \pm 0.5) \times 10^{-4} \text{ cm}^2$. The tunneling mass was assumed to be $0.12m_0$, which is the value for the tunneling mass in the [100] direction.¹ [Equation (7) of Ref. 1 was used with corrections to the asymptotic expansions of the parabolic cylinder functions.]

¹⁰ W. G. Spitzer, F. A. Trumbore, and R. A. Logan, J. Appl. Phys. **32**, 1822 (1961).

¹¹ In Fig. 1 of Ref. 3, a value of $7.5 \times 10^{18}/\text{cm}^3$ had been assumed from resistivity measurements. The new value of $6.7 \times 10^{18}/\text{cm}^3$ was obtained from Hall measurements on the tunneling sample.

The agreement between theory and experiment is probably fortuitous considering the experimental uncertainties and the approximations made in the theory. However, the following appear to be approximations adequate for the description of the Sb-doped Ge units measured in this investigation. (1) The current transfer mechanism is that appropriate to electrons tunneling through an average electrostatic potential which is parabolic, and, at least for doping levels $n_D \sim 7 \times 10^{18} \text{ cm}^{-3}$, fluctuations from this average barrier potential are not important. (2) Specular reflection occurs at the metal-semiconductor interface. (3) The energy levels of the electrons in highly doped *n*-Ge contributing to the tunneling current are given by $\hbar^2 k^2 / 2m_e^*$, where m_e^* is the effective mass of the intrinsic conduction band (or the appropriate generalization for ellipsoidal energy surfaces). This last assumption implies that the Fermi level for *n*-Ge should be at $e\mu_F = (\hbar^2 / 2m_d^*) (\frac{3}{4}\pi^2 n_D)^{2/3}$ above the conduction band edge in the absence of carrier freeze-out (m_d^* is the density-of-states mass = $0.22m_0$ for *n*-Ge). The presence of the sharp minimum in the experimental data at a bias equal to the calculated μ_F (the sharpness of the minimum is due to the improved diode fabrication) is a direct confirmation of this idea. No evidence of a component in the conductance due to band tailing was found.

2. Results for As-doped Ge

Results for vacuum- and air-cleaved samples and a comparison with theory are displayed in Fig. 3. The curve for a vacuum-cleaved sample represents one typical curve out of a total of 10. The curve denoted "air cleaved" represents one out of two almost identical curves. The results shown in Fig. 3 for air- and vacuum-cleaved contacts were obtained from the same single-crystal bar.

The theoretical curves were calculated with the following measured parameters: carrier density $n_D = (5.1 \pm 0.1) \times 10^{18} / \text{cm}^3$, and barrier heights $V_b = 0.63 \pm 0.03 \text{ V}$ and $0.51 \pm 0.03 \text{ V}$ for vacuum- and air-cleaved junctions, respectively. The junction area was $(2.5 \pm 0.5) \times 10^{-4} \text{ cm}^2$. The value $0.12m_0$ was used for the tunneling mass for the calculations.

At present it is not known why the agreement between experiment and theory in absolute value of the conductance-versus-voltage curves is not as good for vacuum-cleaved As-doped junctions as it is for Sb-doped ones. However, the qualitative features of the vacuum-cleaved As-doped Ge data are in good agreement with the theory, and considering the experimental uncertainties in the parameters and the scattering properties of As impurities,⁵ the discrepancies in absolute value are not too surprising. The good agreement between theory and the measured conductance of air-cleaved As-doped junctions is thought to be fortuitous because the phonon structure which is strong in vacuum-cleaved junctions appeared only weakly in air-cleaved junctions (see below).

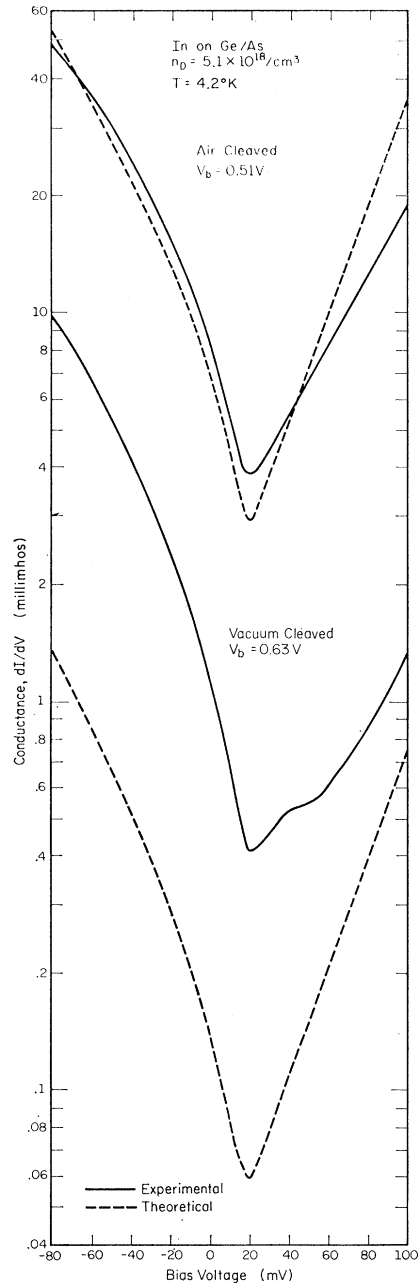


FIG. 3. Comparison between experimental conductance-versus-voltage curves (solid lines) on As-doped Ge at 4.2°K and the conductance calculated using the model developed in Ref. 1 (dashed lines) with In as the contact metal. The lower curves represent a vacuum-cleaved sample for which the barrier height $V_b = 0.63 \text{ V}$. The upper curves represent an air-cleaved sample with $V_b = 0.51 \text{ V}$. Doping level and junction area for both samples are $7.0 \times 10^{18} / \text{cm}^3$ and $2.5 \times 10^{-4} \text{ cm}^2$, respectively. The Fermi degeneracy $\mu_F = 24 \text{ mV}$.

B. Phonon-Assisted Tunneling

In all junctions made with Sb- and As-doped Ge which were fabricated with the vacuum-cleavage technique, strong sharp step increases in the curves of conductance-versus-bias curves were observed at bias

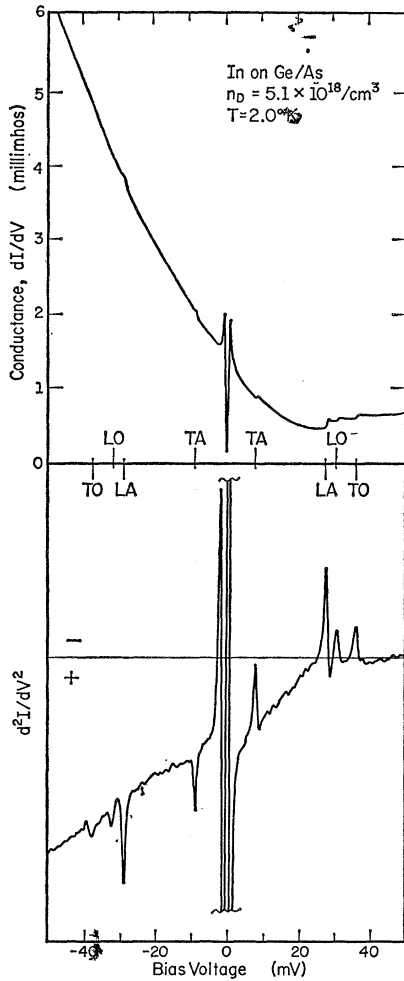


FIG. 4. Conductance and d^2I/dV^2 of an indium contact on As-doped Ge junction at 2°K . The As doping concentration is $n_D = 5.1 \times 10^{18}/\text{cm}^3$. The observation of the In superconducting gap at zero bias is shown explicitly. Its presence shifts the phonon structure to higher energies by $\Delta = 0.5$ mV. Assignment of phonon energies is according to Ref. 4. Sign convention for bias voltage is opposite to that of Ref. 3.

voltages corresponding to the four zone-boundary phonon energies in the $[111]$ direction.⁴ Air-cleaved junctions showed the same type of structure, but very weakly. The chemically prepared units of Ref. 2 showed no such structure.

In Fig. 4, curves of dI/dV and d^2I/dV^2 versus bias are shown for an In contact on vacuum-cleaved As-doped Ge. The temperature was 2°K . Identical structure with nearly the same strength was also found in Sb-doped units. The magnitude of the conductance change at $eV = \pm \hbar\omega_{\text{LA}}$ was approximately $10^{-4} \Omega$ for both Sb- and As-doped vacuum-cleaved units. As is shown in Sec. IV, a conductance increase of this magnitude is expected for the Kleinman mechanism⁶ of LA phonon-assisted tunneling in metal-semiconductor contacts.

IV. LA PHONON-ASSISTED TUNNELING IN n -GE

In this section, we calculate the change $\Delta(dI/dV)$ in the conductance at $eV = \pm \hbar\omega_{\text{LA}}$, where $\hbar\omega_{\text{LA}}$ is the energy of the LA phonon of momentum $\mathbf{q} = (\pi/a)(1,1,1)$. These step increases at $\pm \hbar\omega_{\text{LA}}$ in the conductance are attributed to a mechanism suggested by Kleinman⁶ to explain similar effects in p - n tunnel junctions. For our calculation, there are two important differences between p - n junctions and metal-semiconductor junctions. (1) The electrostatic potential in a p - n junction can be treated as linear in the junction region, whereas in the metal-semiconductor contact, the electrostatic potential near the metal-semiconductor interface is parabolic to a good approximation. (2) The basis functions in a p - n junction are just the complete set of Bloch states in a semiconductor. In the metal-semiconductor contact, we must mix metal and semiconductor basis functions, assuming some type of matching procedure at the interface of the metal and semiconductor.

In Fig. 5, we show a schematic drawing of the band structure of Ge. For n -Ge at $T = 0^\circ\text{K}$, the valence bands are filled and the L_1 conduction band is filled up to an energy $e\mu_F$ above E_{Lc} (for $7 \times 10^{18} \text{ cm}^{-3}$ donors in Ge, $\mu_F = 24$ mV). The subsidiary Γ_2' conduction band is empty. The selection rules for phonon emission¹² are also shown in Fig. 5. The important transition for LA phonons is $\Gamma_2' \leftrightarrow L_1$. The observation of LA phonon emission in the tunneling conductance of our n -Ge units is qualitatively explained as follows.

Consider an applied bias such that electrons are injected from the metal electrode into the Ge electrode ($V < 0$, i.e., metal negative relative to Ge). Most of the current flows by the direct channel in which no phonon emission occurs [Fig. 6(a)]. For tunneling into the (100) face, the four ellipsoids associated with the L_1 conduction band are equivalent, so only one is considered. The metal Fermi surface is large enough to allow direct tunneling without violation of the \mathbf{k}_{\parallel} -conservation rule

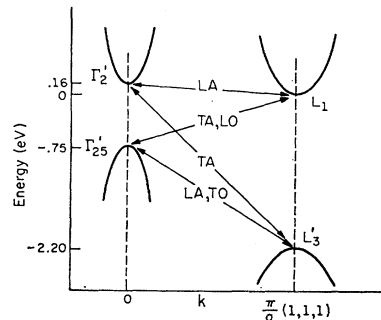


FIG. 5. Simplified model of the band structure for Ge and allowed phonon-assisted transitions between the band extreme (see Ref. 12).

¹² J. J. Tiemann and H. Fritzsche, Phys. Rev. **137**, A1910 (1965); M. Lax and J. J. Hopfield, *ibid.* **124**, 115 (1961).

(specular reflection). This type of tunneling is described by the CDMT theory.¹

Another channel for tunneling is the phonon-assisted tunneling which is a two-step process. Step 1: The first step is the injection of electrons from near the forward direction ($\mathbf{k}_{||} \approx 0$) on the metal Fermi surface into states associated with the Γ_2' conduction band; for the bias voltages of interest, these states are of an energy below the Γ_2' conduction band edge $E_{\Gamma_2'}$, so these states are decaying or evanescent states in the semiconductor [Fig. 6(b)]. The important point made by Kleinman⁶ is that this exponential tail extends well beyond the junction region into the semiconductor $x > d$ (where d is the width of the space-charge region) and is primarily of the Γ_2' symmetry. Hence, there is a rather large region for interaction with phonons. Step 2: The tunneling channel for the electron is completed by the emission of a LA phonon of wave vector $\mathbf{q} \approx (-\pi/a)(1,1,1)$ allowing the electron to make a transition from the state of Γ_2' symmetry to a current-carrying state of symmetry L_1 at $\mathbf{k} = (\pi/a)(1,1,1)$. A similar two-step process occurs when the Ge electrode is biased negative relative to the metal.

It is clear from the conservation of energy that the LA phonon-assisted tunneling can only occur when $eV \geq \hbar\omega_{LA}$ or $eV \leq -\hbar\omega_{LA}$. For example, when electrons are injected from the metal into the Ge, the condition $eV \geq \hbar\omega_{LA}$ must hold if an electron is to emit a phonon of energy $\hbar\omega_{LA}$ and make a transition to an unoccupied state above the Fermi level in the Ge electrode.

Let us now calculate quantitatively the change $\Delta(dI/dV)$ in the conductance at $eV = \pm \hbar\omega_{LA}$. For simplicity, we follow Kleinman⁶ and calculate only that contribution which comes from the interaction occurring in the region $x > d$. The contribution from the region $x < d$ should be smaller than that for $x > d$ because the symmetry of the wave function is predominantly hole-like near $x = 0$ (Γ_{25}' symmetry).

The Bloch states for \mathbf{k}_r near $\mathbf{k}_0 = (\pi/a)(1,1,1)$ with energy $E_{\mathbf{k}_r}$ near E_{L_1} (energy of L_1 state at \mathbf{k}_0) can be written as^{6,13}

$$\Psi_{\mathbf{k}_r} = e^{i(\mathbf{k}_r - \mathbf{k}_0) \cdot \mathbf{r}} u_{L_1}(\mathbf{r}), \quad x > d \quad (4.1)$$

where $u_{L_1}(\mathbf{r})$ is the Bloch function at \mathbf{k}_0 with L_1 symmetry. The states of symmetry Γ_2' associated with $\mathbf{k} = 0$ and energy $E_{\Gamma_2'}$ are written as^{6,13}

$$\Psi_{\mathbf{k}_l} = \beta(x) e^{i\mathbf{k}_{||} \cdot \mathbf{r}} u_{\Gamma_2'}(\mathbf{r}), \quad x > 0. \quad (4.2)$$

$u_{\Gamma_2'}(\mathbf{r})$ is the Bloch function at $\mathbf{k} = 0$ with Γ_2' symmetry and energy $E_{\Gamma_2'}$. The envelope function $\beta(x)$ is a solution to ($x > 0$)

$$-\left(\frac{\hbar^2}{2m_{\Gamma_2'}}\right)(d^2\beta/dx^2) + V(x)\beta = (E_{\mathbf{k}_l} - E_{\Gamma_2'} - \hbar^2 k_{||}^2 / 2m_{\Gamma_2'})\beta. \quad (4.3)$$

¹³ J. M. Luttinger and W. Kohn, Phys. Rev. **97**, 869 (1955). (Additional references can be found in this reference.)

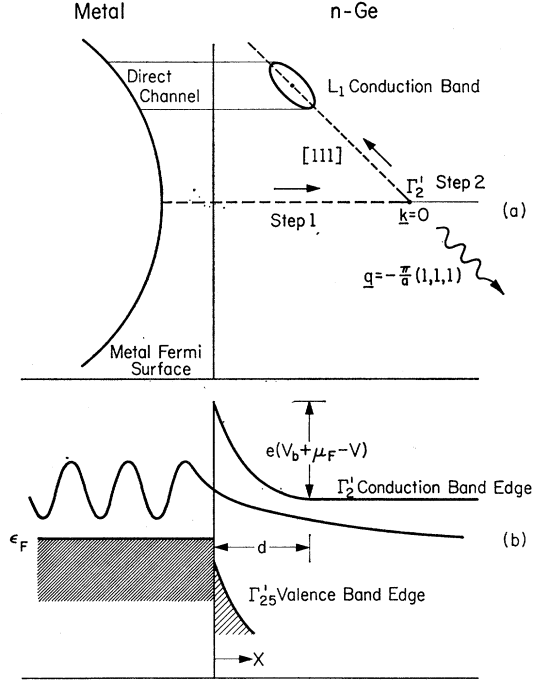


FIG. 6. (a) Schematic representation of metal-Ge (n -type) interface in k -space. One-electron tunneling flows via direct channel. Phonon-assisted tunneling involves two-step process. For reverse bias, step 1 is the injection of an electron from the metal Fermi surface into an evanescent semiconductor state associated with the Γ_2' conduction band. Step 2 is the emission of a Ge phonon of momentum $\mathbf{q} \approx -(\pi/a)(1,1,1)$ and the transition of the electron to a current-carrying state in the L_1 conduction band. A similar process occurs in forward bias. (b) The metal- Γ_2' envelope function. Metal wave function connects onto an evanescent semiconductor state associated with Γ_2' conduction band.

The effective mass of the Γ_2' conduction band is denoted by $m_{\Gamma_2'}$ and the electrostatic potential⁹ is

$$V(x) = (2\pi e^2 n_D / \epsilon_s)(x-d)^2, \quad d > x > 0 \\ = 0, \quad x > d. \quad (4.4)$$

The number of donors per unit volume is n_D , the static dielectric constant of the semiconductor is ϵ_s , and d is given by (in the parabolic potential approximation)⁹

$$eV_b + e\mu_F - eV = 2\pi e^2 n_D d^2 / \epsilon_s, \quad (4.5a)$$

$$d = [(\epsilon_s / 2\pi e n_D)(V_b + \mu_F - V)]^{1/2}, \quad (4.5b)$$

where V_b is the barrier height.

Equation (4.3) is valid if $eV_b \lesssim \frac{1}{2} E_g$ where E_g is the direct gap. Since $eV_b = 0.63$ eV and $E_g = .95$ eV, we see that Eq. (4.3) will not be valid for x near 0. We will account for this in our final expression for $\Delta(dI/dV)$ by estimating the influence of the valence band with a two-band model. However, for simplicity let us initially assume that Eq. (4.3) is valid for all $x > 0$.

To completely specify $\beta(x)$, we must match $\beta(x)$ at $x = 0$ to the envelope function in the metal which is of the form

$$\beta(x) = 2^{1/2} \sin(k_{lx}x + \delta), \quad x < 0 \quad (4.6)$$

where δ is a phase angle and $k_{lx} \simeq k_F$, the metal Fermi radius, for the states of interest. We require continuity of $\beta(x)$ and $(1/m^*)d\beta/dx$ at $x=0$.¹⁴ We also assume \mathbf{k}_{ll} conservation (specular reflection).

The notation employed is that \mathbf{k}_r represents the L_1 current carrying states and \mathbf{k}_l the metal- Γ_2' states.

We note that for $x > d$,

$$\beta(x) = \beta(d)e^{-K_{\Gamma c}(x-d)}, \quad (4.7)$$

where

$$K_{\Gamma c} = \left[k_{ll}^2 + \frac{2m_{\Gamma c}}{\hbar^2}(E_{\Gamma c} - E_{kl}) \right]^{1/2}. \quad (4.8)$$

For the calculation of $\Delta(dI/dV)$ we will be interested in the case ($eV = \pm \hbar\omega_{LA}$)

$$E_{kl} = -eV + e\mu_F. \quad (4.9)$$

Following CDMT,¹ we write $\beta(x)$ as

$$\beta(x) = AU(a, \eta) + BV(a, \eta), \quad (4.10)$$

where

$$a = \lambda^2 \left(k_{ll}^2 + \frac{2m_{\Gamma c}}{\hbar^2}(E_{\Gamma c} - E_{kl}) \right) = \lambda^2 K_{\Gamma c}^2, \quad (4.11a)$$

$$\lambda = (\hbar^2 \epsilon_s / 16\pi m_{\Gamma c} e^2 n_D)^{1/4}, \quad (4.11b)$$

$$\eta = (d-x)/\lambda. \quad (4.11c)$$

A and B are constants to be determined by matching $\beta(x)$ at $x=0$ and $x=d$, and $U(a, \eta)$ and $V(a, \eta)$ are parabolic cylindrical functions.¹⁵ $V(a, \eta)$ is the exponentially increasing function as $\eta \rightarrow \infty$, and $U(a, \eta)$ is the exponentially decreasing function as $\eta \rightarrow \infty$.

Applying the matching conditions and neglecting $U(a, \eta_d)$ compared to $V(a, \eta_d)$, where

$$\eta_d = d/\lambda, \quad (4.12)$$

we find

$$|\beta(d)|^2 = 4(2\pi)^{1/2} \lambda K(0) \exp\left(-2 \int_0^d K dx\right) / \Gamma\left(\frac{1}{2} + a\right) \left[1 + \left(\frac{m_0 K(0)}{m_{\Gamma c} k_F} \right)^2 \right] (U'(a, 0) - a^{1/2} U(a, 0))^2, \quad (4.13)$$

where

$$K^2(x) = k_{ll}^2 + \frac{2m_{\Gamma c}}{\hbar^2}(E_{\Gamma c} - E_{kl} + V(x)), \quad (4.14)$$

and the metal electron mass is taken to be the free-electron mass m_0 .

We have made use of Darwin's asymptotic expansion¹⁵ for $V(a, \eta)$ in Eq. (4.14) in place of the asymptotic

¹⁴ D. J. BenDaniel and C. B. Duke, Phys. Rev. **152**, 683 (1966).

¹⁵ J. C. P. Miller, in *Handbook of Mathematical Functions*, edited by M. Abramowitz and I. A. Stegun (U. S. Department of Commerce, National Bureau of Standards, Washington, D. C., 1964), Appl. Math. Ser. 55, p. 685.

form used in CDMT¹ because the former is more closely related to the WKB approximation.

To take account of the influence of the valence band and the breakdown of Eq. (4.3) near $x=0$, we replace $K(x)$ above with the expression obtained for a trajectory in a two-band model⁹ (for $\mathbf{k}_{ll}=0$),

$$K(x) = \left\{ (2m^*/\hbar^2 E_0) [V(x) - E_{kl} + E_{\Gamma c}] \times [E_0 - V(x) + E_{kl} - E_{\Gamma c}] \right\}^{1/2}, \quad (4.15a)$$

where

$$1/m^* = \frac{1}{2}(m_{\Gamma c}^{-1} + m_v^{-1}). \quad (4.15b)$$

The effective mass of the light hole valence band is m_v . We find

$$\int_0^d K dx = \frac{C}{3} \left\{ (\zeta - 2\epsilon) E(\varphi, k) + \epsilon F(\varphi, k) + (\alpha + 3\epsilon - \zeta) [\alpha(\zeta - \epsilon - \alpha)/\zeta(\alpha + \epsilon)]^{1/2} \right\}, \quad (4.16a)$$

where

$$\begin{aligned} \alpha &= (V_b + \mu_F - V)/\mu_F, & \zeta &= E_0/\mu_F, \\ \epsilon &= (E_{\Gamma c} - E_{kl})/\mu_F, & \sin \varphi &= [\alpha\zeta/(\zeta - \epsilon)(\alpha + \epsilon)]^{1/2}, \end{aligned} \quad (4.16b)$$

$$C = \mu_F/E_0, \quad k = [(\zeta - \epsilon/s)\zeta]^{1/2},$$

$$E_0 = (\hbar^2 \pi e^2 n_D / m^* \epsilon_s)^{1/2},$$

E and F are incomplete elliptic integrals. We note that our result differs from that of Conley and Mahan⁹ because no turning point occurs between $0 \leq x \leq d$.

Let us now calculate the transition rate for a transition from Ψ_{kl} to Ψ_{kr} with the emission of a LA phonon of wave vector \mathbf{q} :

$$\begin{aligned} P_{kl, kr}(\mathbf{q}) &= \frac{2\pi}{\hbar} |\langle \Psi_{kl} | H_{eL-ph}(\mathbf{q}) | \Psi_{kr} \rangle|^2 \\ &\quad \times \delta(E_{kl} - E_{kr} - \hbar\omega_{LA}), \end{aligned} \quad (4.17a)$$

$$\begin{aligned} &= \frac{2\pi}{\hbar} |\beta(d)|^2 M_{LA}^2 \left| \int_d^\infty dx e^{-K_{\Gamma c}(x-d)} e^{iq_x x} e^{ik_{rx} x} \right|^2 \\ &\quad \times \delta_{k_{ll}, q_{ll} + k_{rll}} \delta(E_{kl} - E_{kr} - \hbar\omega_{LA}), \end{aligned} \quad (4.17b)$$

$$\begin{aligned} &= \frac{2\pi}{\hbar} \frac{|\beta(d)|^2 M_{LA}^2}{(q_x + k_{rx})^2 + K_{\Gamma c}^2} \\ &\quad \times \delta_{k_{ll}, q_{ll} + k_{rll}} \delta(E_{kl} - E_{kr} - \hbar\omega_{LA}). \end{aligned} \quad (4.17c)$$

The matrix element M_{LA} is defined as

$$M_{LA} = \langle u_{\Gamma c} | H_{eL-ph}(\mathbf{k}_0) | u_{Lc} \rangle. \quad (4.18)$$

We use normalization in a unit volume, neglect dispersion in the phonon energy $\hbar\omega_{LA}$, and consider only the contribution from $x > d$.

To be completely rigorous, we should have taken the L_1 states to be standing waves in place of running waves and we should have taken account of the boundary in the phonon mode description. To the extent that we average over \mathbf{k} and \mathbf{q} in calculating the conductance, such essentially interference effects should vanish.

For $V < 0$, the current due to this mechanism at $T = 0^\circ\text{K}$ is

$$I = -8eA \sum_{\mathbf{k}_l, \mathbf{k}_r, \mathbf{q}} P_{\mathbf{k}_l, \mathbf{k}_r}(\mathbf{q}) f(\mathbf{k}_l) [1 - f(\mathbf{k}_r)], \quad (4.19)$$

where $f(\mathbf{k})$ is the Fermi function and A is the area of the junction. The factor 8 arises from the two spin directions and the four conduction-band minima in Ge.

Performing the sum over \mathbf{q} , we find

$$\begin{aligned} & \sum_{\mathbf{q}} P_{\mathbf{k}_l, \mathbf{k}_r}(\mathbf{q}) \\ &= (2\pi/\hbar) |\beta(d)|^2 M_{\text{LA}}^2 (1/2K_{\Gamma_c}) \\ & \quad \times \delta(E_{\mathbf{k}_l} - E_{\mathbf{k}_r} - \hbar\omega_{\text{LA}}). \end{aligned} \quad (4.20)$$

We see that $\sum_{\mathbf{q}} P_{\mathbf{k}_l, \mathbf{k}_r}(\mathbf{q})$ depends on the variables $E_{\mathbf{k}_l}$, $E_{\mathbf{k}_r}$, and k_{l11} [$\beta(d)$ and K_{Γ_c} depend upon k_{l11}], so we write

$$\begin{aligned} I = & - \frac{8eAM_{\text{LA}}^2}{\hbar^2 v_F} \int dE_{\mathbf{k}_l} f(E_{\mathbf{k}_l} + eV - e\mu_F) \\ & \times \int dE_{\mathbf{k}_r} \rho(E_{\mathbf{k}_r}) [1 - f(E_{\mathbf{k}_r} - e\mu_F)] \\ & \times \delta(E_{\mathbf{k}_l} - E_{\mathbf{k}_r} - \hbar\omega_{\text{LA}}) \int \frac{d^2 k_{l11}}{(2\pi)^2} \frac{|\beta(d)|^2}{K_{\Gamma_c}}, \end{aligned} \quad (4.21)$$

where $\rho(E)$ is the Ge density of states for one spin-band and one conduction-band minimum at L_1 . The energy variable $E_{\mathbf{k}_l}$ is the total energy, including potential energy, measured relative to the L_1 conduction band edge. The Fermi velocity of the metal is $v_F = \hbar k_F / m_0$.

Doing the $E_{\mathbf{k}_r}$ integration, we find

$$\begin{aligned} I = & - \frac{8eAM_{\text{LA}}^2}{\hbar^2 v_F} \int dE_{\mathbf{k}_l} \rho(E_{\mathbf{k}_l} - \hbar\omega_{\text{LA}}) f(E_{\mathbf{k}_l} + eV - e\mu_F) \\ & \times [1 - f(E_{\mathbf{k}_l} - \hbar\omega_{\text{LA}} - e\mu_F)] \int \frac{d^2 k_{l11}}{(2\pi)^2} \frac{|\beta(d)|^2}{K_{\Gamma_c}}. \end{aligned} \quad (4.22)$$

We are interested in the conductance dI/dV , which is given by

$$\begin{aligned} \frac{dI}{dV} = & \frac{8e^2 AM_{\text{LA}}^2}{\hbar^2 v_F} \rho(e\mu_F - eV - \hbar\omega_{\text{LA}}) \\ & \times [1 - f(-eV - \hbar\omega_{\text{LA}})] \int \frac{d^2 k_{l11}}{(2\pi)^2} \frac{|\beta(d)|^2}{K_{\Gamma_c}}. \end{aligned} \quad (4.23)$$

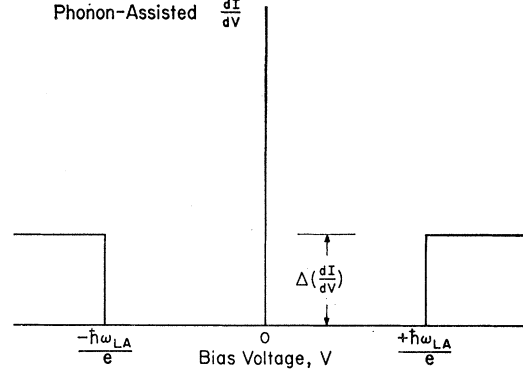


FIG. 7. The component of the conductance due to LA phonon-assisted tunneling.

In Eq. (4.23), we have taken a derivative of the Fermi function only. The $E_{\mathbf{k}_l}$ variable in the expressions for $|\beta(d)|^2$ and K_{Γ_c} [Eqs. (4.8) and (4.13)] is evaluated at $e\mu_F - eV$. The k_{l11} integration can be extended to infinity.

We see from Eq. (4.23) that dI/dV vanishes for $-\hbar\omega_{\text{LA}} < eV < 0$, and has a step increase at $eV = -\hbar\omega_{\text{LA}}$ (see Fig. 7)

$$\Delta\left(\frac{dI}{dV}\right) = \frac{8e^2 AM_{\text{LA}}^2 \rho(e\mu_F)}{\hbar^2 v_F} \int \frac{d^2 k_{l11}}{(2\pi)^2} \frac{|\beta(d)|^2}{K_{\Gamma_c}}, \quad (4.24)$$

where $E_{\mathbf{k}_l}$ is evaluated at $e\mu_F + \hbar\omega_{\text{LA}}$. Similarly, for $V > 0$, we find dI/dV vanishes for $0 < eV < \hbar\omega_{\text{LA}}$ and has a step increase at $eV = \hbar\omega_{\text{LA}}$ given by Eq. (4.24) with $E_{\mathbf{k}_l}$ evaluated at $e\mu_F - \hbar\omega_{\text{LA}}$.

The most important k_{l11} dependence of $|\beta(d)|^2/K_{\Gamma_c}$ is in the WKB exponential $\int_0^d K(k_{l11}, x) dx$ [previously we have suppressed the variable k_{l11} in $K(x)$], where

$$K(k_{l11}, x) = [K^2(x) + k_{l11}^2]^{1/2}. \quad (4.25)$$

In Eq. (4.25), $K(x)$ is given by Eq. (4.15). We estimate the k_{l11} integral in Eq. (4.24) by expanding the WKB exponent to order k_{l11}^2 and neglecting all other k_{l11} dependences. Hence, to a reasonable approximation,

$$\int \frac{d^2 k_{l11}}{(2\pi)^2} \frac{|\beta(d)|^2}{K_{\Gamma_c}} \simeq \frac{k_a^2}{4\pi} \left(\frac{|\beta(d)|^2}{K_{\Gamma_c}} \right)_0, \quad (4.26a)$$

where

$$\frac{1}{k_a^2} = \int_0^d [K(x)]^{-1} dx, \quad (4.26b)$$

and

$$\left(\frac{|\beta(d)|^2}{K_{\Gamma_c}} \right)_0 = \left(\frac{|\beta(d)|^2}{K_{\Gamma_c}} \right)_{k_{l11}=0}. \quad (4.26c)$$

From Eq. (4.15), we find

$$1/k_a^2 = \hbar^2 F(\varphi, k) / 2m^* E_0, \quad (4.27)$$

where the definitions in Eq. (4.16b) apply.

TABLE I. Parameters for LA phonon-assisted tunneling.

$n_D = 7 \times 10^{18} \text{ cm}^{-3}$	$A = 2.5 \times 10^{-4} \text{ cm}^2$
$\epsilon_s = 16$	$\hbar\omega_{LA} = 28 \text{ meV}$
$m_{\Gamma_c} = 0.034m_0$	$M_{LA}^2 = 4.3 \times 10^{-49} \text{ erg}^2 \text{ cm}^3$
$m_v = 0.044m_0$	$v_F = 1.7 \times 10^8 \text{ cm/sec}$
$m^* = 0.038m_0$	$E_{\Gamma_c} - E_{L_c} = 0.154 \text{ eV}$
$\mu_F = 24 \text{ mV}$	$E_{L_c} - E_{L_v} = 2.36 \text{ eV}$
$V_b = 0.63 \text{ V}$	
$E_g = 0.91 \text{ eV}$ (Direct gap)	

Hence, we find that the step increase in the conductance at $eV = \pm \hbar\omega_{LA}$ is given by

$$\Delta\left(\frac{dI}{dV}\right) = \frac{2e^2 A M_{LA}^2 \rho(e\mu_F) k_a^2}{\pi \hbar^2 v_F} \left(\frac{|\beta(d)|^2}{K_{\Gamma_c}} \right)_0. \quad (4.28)$$

Using the parameters listed in Table I,¹⁶ we find that (ignoring small differences between forward and reverse bias due to the changing space-charge region)

$$\Delta(dI/dV) \simeq 10^{-4} \Omega^{-1}, \quad (4.29)$$

which is in order-of-magnitude agreement with the experimental data for vacuum-cleaved Sb-doped Ge units. [The predicted size of the effect for vacuum-cleaved As-doped units ($n_D = 5.1 \times 10^{18}/\text{cm}^3$) is an order of magnitude lower than that observed, which is also the case for the background conductance in Fig. 3.] Since the background conductance $\sim 10^{-3} \Omega^{-1}$, the step increases for LA phonon-assisted tunneling are approximately 10% of the background which makes them easily detectable.

V. PHONON-ASSISTED TUNNELING DUE TO TA, LO, AND TO PHONON EMISSION

We have given a detailed analysis of only the LA phonon-assisted tunneling because accurate values for the electron-phonon matrix elements have been given only for the LA¹⁶ phonon between states of symmetry Γ_2' and L_1 . In this section, we shall make qualitative estimates of the phonon-assisted tunneling due to TA, LO, and TO phonon emission.

The strength of the TA phonon-assisted tunneling (conductance change at $eV = \pm \hbar\omega_{TA}$) can be estimated if it is assumed that $M_{TA} = M_{LA}$ (as done, for example, in Ref. 10) and if the important region for the electron-phonon interaction is near, but not in the Schottky-barrier region ($x > d$). Since a typical energy of the metal- Γ_2' states is $E_{\Gamma_c} - E_{L_c} - e\mu_F$ below the Γ_2' conduction band edge, the Γ_2' tail contains some Γ_{25}'

character. The magnitude of the Γ_{25}' admixture relative to Γ_2' is approximately $(E_{\Gamma_c} - E_{L_c} - e\mu_F)/E_g \simeq 0.14$. (E_g is the direct gap at $\mathbf{k} = 0$). Since the $\Gamma_{25}' \leftrightarrow L_1$ transition is allowed for TA phonons (see Fig. 5) and there are two transverse phonon branches, the change in conductance at $eV = \pm \hbar\omega_{TA}$ should be about 2×0.14 or $\sim 30\%$ of that at $eV = \pm \hbar\omega_{LA}$. From Fig. 4, we see that this rough estimate is reasonable. We have neglected the contribution from the electron-phonon interaction in the Schottky-barrier region ($0 < x < d$) and have neglected the contribution from the admixture of L_3' into the L_1 conduction band states, which is $\sim e\mu_F/(E_{L_c} - E_{L_v}) \approx 10^{-2}$. ($E_{L_c} - E_{L_v}$ is the energy gap between L_1 and L_3'). The allowed transition $\Gamma_2' \leftrightarrow L_3'$ should therefore contribute to the TA phonon-assisted tunneling only $\sim 1\%$ as much as the $\Gamma_{25}' \leftrightarrow L_1$ if the relevant matrix elements are comparable.

The strength of the LO phonon-assisted tunneling can be compared to the strength of the TA phonon-assisted tunneling since the $\Gamma_{25}' \leftrightarrow L_1$ transition is allowed for both LO and TA phonons (Fig. 5). If the matrix element for LO phonon emission is the same as for TA phonon emission, then the change in conductance at $eV = \pm \hbar\omega_{LO}$ should be about half of that at $eV = \pm \hbar\omega_{TA}$ since there is only one longitudinal branch. This rough estimate is also in reasonable agreement with the experimental results (Fig. 4). [As before, we neglect the LO contribution from the $\Gamma_2' \leftrightarrow L_3'$ transition ($\sim 1\%$).]

The estimated strength of the TO relative to the LO phonon-assisted tunneling is, however, not in good agreement with the experimental results. The allowed transition for TO phonons is $\Gamma_{25}' \leftrightarrow L_3'$, whereas the allowed transition for LO phonons is $\Gamma_{25}' \leftrightarrow L_1$ (Fig. 5). If the matrix elements for these two transitions are comparable, we would expect the strength of the TO relative to the LO to be $2e\mu_F/(E_{L_c} - E_{L_v})$, or $\sim 2\%$. From Fig. 5, we see that the experimental data show that the TO phonon-assisted tunneling is comparable to the LO phonon-assisted tunneling, not 50 times smaller. We are, therefore, forced to conclude that either the TO matrix element is nearly an order of magnitude larger than the LO matrix element, or that the TO phonon-assisted tunneling proceeds by a mechanism which does not obey the selection rules, such as scattering from crystal imperfections.

VI. SUMMARY

One group of metal-Ge (*n*-type) tunnel junctions studied in this investigation were fabricated by cleaving Ge crystals in vacuum and then evaporating metal electrodes (In or Pb) through a metal mask onto the cleaved surface. For junctions which were made from Sb-doped Ge ($n \simeq 7 \times 10^{18} \text{ cm}^{-3}$), it was found that the experimentally measured curves of conductance versus bias voltage agreed in shape and magnitude with the predictions of the one-electron Schottky-barrier¹ model where all

¹⁶ Values of the parameters can be found in Refs. 16 and 12. The phonon energy $\hbar\omega_{LA}$ has been accurately measured by R. T. Payne, Ref. 4. The value for M_{LA}^2 is due to E. O. Kane [J. Appl. Phys. **32**, 83 (1961)], who analyzed the optical absorption data of G. G. Macfarlane, T. P. McLean, J. E. Quarrington, and V. Roberts [Phys. Rev. **108**, 1377 (1957)]. Typical values of v_F can be found in W. J. Tomasch, Phys. Rev. Letters **16**, 16 (1966). The separation $E_{\Gamma_c} - E_{L_c}$ has been measured by Conley and Tiemann, Ref. 2.

parameters were determined from experiments other than tunneling.

Such agreement, although somewhat fortuitous, showed that the following approximations or assumptions are adequate in the description of these tunnel junctions. (1) The electrostatic potential near the metal-semiconductor interface can be replaced by an average parabolic potential. (2) Specular reflection occurs at the interface. (3) The energy levels of the highly doped degenerate *n*-type Ge are given by $\hbar^2 k^2 / 2m_c^*$ (or an appropriate generalization for ellipsoidal energy surfaces) and at $T=0^\circ\text{K}$ these states are filled up to $e\mu_F$ above the conduction band edge.

The conductance curves for vacuum-cleaved As-doped units do not agree with theory in magnitude as well as the Sb-doped units, but the qualitative features are similar. This discrepancy is not understood at present.

Capacitance measurements have been made on both vacuum-cleaved and air-cleaved junctions. For vacuum-cleaved units, the barrier height was found to be $V_b = 0.63$ V and for air-cleaved, $V_b = 0.51$ V. A substantially higher conductance due to the lower barrier height was observed in the air-cleaved junctions which formed the second group of junctions studied. The measured barrier heights were independent of the contact metal (In or Pb) and of the semiconductor impurity (Sb or As).

Strong phonon-assisted tunneling was observed in both Sb-doped and As-doped vacuum-cleaved units. Air-cleaved units showed only weak phonon-assisted tunneling. Prominent step increases in the conductance of vacuum-cleaved junctions were observed at bias $eV = \pm \hbar\omega$, where $\hbar\omega$ is the energy of a Ge zone-boundary phonon along the $[111]$ direction. Structure associated with the LA phonon was the strongest. The TA phonon structure was not as strong as that for the LA phonons. The structure for the LO and the TO phonons was somewhat weaker than the structure for the acoustic phonons, but still clearly observable in dI/dV .

A calculation of the LA phonon-assisted tunneling has been presented in Sec. IV. The predicted strength of the step increases in the conductance at $eV = \pm \hbar\omega_{\text{LA}}$ is of the same order of magnitude as that observed experimentally. The calculation is based upon a modifica-

tion of Kleinman's⁶ explanation of similar phenomena in Ge *p-n* junctions. The essential feature of the mechanism is a two-step process, where (in reverse bias), an electron is injected from the metal into an evanescent semiconductor state associated with the Γ_2' conduction band and then emits a LA phonon with $\mathbf{q} \simeq -(\pi/a)-(1,1,1)$, making a transition to a current-carrying state at L_1 . A similar process occurs at forward bias. Since this is an inelastic emission process, the conductance has a symmetric (with respect to zero-bias) threshold characteristic which is clearly seen in the experimental data.

A qualitative analysis of the phonon-assisted tunneling due to TA, LO, and TO phonon emission has been given in Sec. V. The relative strengths of the conductance changes at $eV = \pm \hbar\omega$ ($\omega = \omega_{\text{TA}}$, ω_{LO} , or ω_{TO}) were found to be reasonable for TA and LO phonons assuming the appropriate electron-phonon matrix elements are comparable. The strength of the TO phonon emission, however, is experimentally nearly 50 times larger than expected. This strong TO phonon-assisted tunneling is not understood.

It should be pointed out that the mechanism for phonon-assisted tunneling described in this paper (with the possible exception of the TO phonons), is due to the coherent coupling of the tunneling electrons to the constituent atoms of the semiconductor electrode and is not due to incoherent impurity-induced coupling.¹⁷

Finally, it should be noted that the sharp strong structure in d^2I/dV^2 at $eV = \pm \hbar\omega$ provides an accurate method of measuring the phonon energies. The pronounced minimum in the conductance at $V = \mu_F$ gives a reasonable estimate of the Fermi degeneracy. So the metal-semiconductor tunnel junction prepared by the vacuum-cleavage technique provides a useful spectrographic tool.³

ACKNOWLEDGMENTS

The authors would like to acknowledge Miss L. Roth of Purdue University for the supply of Sb-doped samples, Professor C. T. Sah for the use of an rf admittance bridge, and Professor W. D. Compton and Professor C. B. Duke for useful discussions.

¹⁷ C. B. Duke, S. D. Silverstein, and A. J. Bennett, Phys. Rev. Letters **19**, 312 (1967); Phys. Rev. **176**, 969 (1968).